JOURNAL OF GUIDANCE, CONTROL, AND DYNAMICS
Vol. 30, No. 2, March–April 2007

Nonlinear Black-Box Modeling of Aeroelastic Systems Using Structure Detection: Application to F/A-18 Data

Sunil L. Kukreja* and Martin J. Brenner
NASA Dryden Flight Research Center, Edwards, California 93523-0273

DOI: 10.2514/1.20835

Structure detection is a procedure for selecting a subset of candidate terms, from a full model description, that best describes the observed output. This is a necessary procedure to compute an efficient system description which may afford greater insight into the functionality of the system or a simpler controller design. Structure computation as a tool for "black-box" modeling is not well known to the flight-test community but may be of critical importance in the development of robust, parsimonious models. Moreover, this approach may lead to efficient strategies for rapid envelope expansion which may save significant development time and costs. Structure detection methods applicable to nonlinear autoregressive, moving average exogenous modeling are applied to aeroelastic dynamics and their properties demonstrated via continuous-time simulations of experimental conditions. Simulation results from a nonlinear dynamic model of aircraft structural free-play demonstrate that methods developed for nonlinear autoregressive, moving average exogenous structure computation provide a high degree of accuracy for selection of the exact model structure from an overparameterized model description. Applicability of these methods to the F/A-18 active aeroelastic wing using flight-test data is shown by identifying a parsimonious system description with a high percent fit for cross-validated data.

I. Introduction

THE behavior of many nonlinear dynamic systems can be represented as an expansion of its present output value in terms of present and past values of the input signal, past values of the output signal, and past values of the innovation, represented as a discrete-time polynomial [1–3]. A system modeled in this form is popularly known as a NARMAX (nonlinear autoregressive, moving average exogenous) model and is linear in the parameters. When fully expanded, this system representation yields a large number of possible terms which may be required to represent the dynamic process [4]. In practice, many of these candidate terms are insignificant and, therefore, can be removed. Consequently, the structure detection problem is that of selecting a subset of candidate terms that best predicts the output while maintaining an efficient system description.

There are two fundamental approaches to the structure detection problem: 1) exhaustive search, where every possible subset of the full model is considered (see, e.g., [5,6]), or 2) parameter variance, where the covariance matrix, P_θ, based on input–output data and estimated residuals is used to assess parameter relevance (see, e.g., [7]). Both have problems. Exhaustive search requires a large number of computations whereas parameter variance estimates are often inaccurate when the number of candidate terms is large.

System identification, or black-box modeling, is a critical step in aircraft development, analysis, and validation for flight worthiness. The development and testing of aircraft typically takes many years and requires considerable expenditure of limited resources. One reason for lengthy development time/costs is inadequate knowledge of an appropriate model type or structure to use for parameter estimation. Selection of an insufficient model structure may lead to difficulties in parameter estimation, giving estimates with significant biases and/or large variances [8]. This often complicates control synthesis or renders it infeasible. The power of using NARMAX structure detection techniques as a tool for model development (i.e., black-box modeling) is that it can provide a parsimonious system description which can describe complex aeroelastic behavior over a large operating range. Consequently, this provides models that can be more robust and, therefore, reduce development time.

Recently, Kukreja and Brenner [9] showed that NARMAX identification is well suited to describing aeroelastic phenomena. However, in their study the model structure was assumed fully known utilizing basic principles governing the equations of motion [10,11]. When studying aeroelastic systems it may not be practical to assume that the exact model structure is well known a priori. In aerospace systems analysis one of the main objectives is not only to estimate system parameters but to gain insight into the structure of the underlying system. Therefore, structure computation is of significant relevance and importance to modeling and design of aircraft and aerospace vehicles. Structure computation may indicate deficiencies in an analytical model and could lead to improved modeling strategies and also provide a parsimonious, black-box, system description for control synthesis [12].

In this paper, we investigate the applicability of NARMAX structure detection methods to 1) a simulated model of aircraft freeplay and 2) F/A-18 active aeroelastic wing (AAW) flight-test data. Our results show that NARMAX structure detection techniques provide a high degree of accuracy for selection of the exact model structure with simulated data. Analysis of experimental flight-test data provides a parsimonious system description with a high percent fit for cross-validated data. Overall, this paper contributes to the understanding of the use of NARMAX structure detection techniques for black-box modeling of nonlinear aerospace systems.

The organization of this paper is as follows. The NARMAX model structure is described in Sec II. Section III summarizes an estimation technique appropriate for NARMAX model identification whereas Sec. IV reviews commonly used techniques for assessing parameter significance. In Sec. V a continuous-time representation of a nonlinear model describing aircraft dynamics is given and its NARMAX representation is derived. Simulation results of several NARMAX structure detection algorithms are presented in Sec. VI whereas Sec. VII illustrates application to experimental AAW data. Section VIII provides a discussion of our findings and Sec. IX summarizes the conclusions of our study.

Received 31 October 2005; revision received 3 March 2006; accepted for publication 7 March 2006.

*Structural Dynamics Group, Aerostructures Branch, MailStop 4820 2A; sunil.kukreja@nasa.gov (corresponding author).

II. NARMAX Model Form

Kolmogorov–Gabor polynomials have been well known in control engineering for many years [3,13]. However, these equations have recently been popularized by Billings and coworkers [1,2] for use in identification, modeling, and control. The NARMAX structure is a general parametric form for modeling nonlinear systems [1]. This so-called NARMAX structure describes both the stochastic and deterministic components of nonlinear systems. Many nonlinear systems are a special case of the general NARMAX structure [14]. The NARMAX structure models the input–output relationship as a nonlinear difference equation of the form

$$z(n) = f[z(n-1), \ldots, z(n-n_z), u(n), \ldots, u(n-n_u), e(n-1), \ldots, e(n-n_e)] + e(n) \quad (1)$$

f denotes a nonlinear mapping, u is the controlled or exogenous input, z is the measured output, and e is the uncontrolled input or innovation. For the special case where f is a nonlinear mapping of polynomial form it may include a variety of nonlinear terms, such as terms raised to an integer power [e.g., $u^3(n-3)$], products of present and past inputs [e.g., $u(n)u(n-2)$], past outputs [e.g., $z^2(n-3)z(n-5)$], or cross terms [e.g., $u(n-1)z^2(n-3)$]. In general, the nonlinear mapping f can be described by a wide variety of nonlinear functions such as sigmoids or splines [14,15].

For simplicity of the present discussion, we assume nonlinearities that can be described by a polynomial expansion. Consider the following NARMAX model that is described by a polynomial expansion as

$$z(n) = \theta_1 z^2(n-2) + \theta_2 u^3(n-1) + \theta_3 u^2(n-1)u(n-2) + \theta_4 z(n-2)e(n-2) + \theta_5 e^2(n-2) + e(n) \quad (2)$$

This model contains a variety of nonlinear terms (regressors) but is *linear in the parameters* and, therefore, pseudolinear regression techniques can be used for parameter estimation [6,16–18].

The order of a polynomial class NARMAX model may be defined as

$$O = [n_u n_z n_e l] \quad (3)$$

where n_u is the maximum input lag, n_z the maximum output lag, n_e the maximum error lag, and l the maximum nonlinearity order. For a nonpolynomial class NARMAX model, l is simply replaced by an appropriate basis function. The maximum number of terms in a NARMAX model with n_u, n_z, and n_e dynamic terms and lth order nonlinearity is [17]

$$p = \sum_{i=1}^{l} p_i + 1; \qquad p_i = \frac{p_{i-1}(n_u + n_z + n_e + i)}{i}, \qquad p_0 = 1 \quad (4)$$

For nonlinear systems, output additive noise can produce multiplicative terms between input, output, and itself. To compute unbiased parameter estimates a noise model needs to be estimated. As a result, the number of candidate terms can become large for even moderately complex models making structure detection difficult. For example, consider model (2), which is of order $O = [2\,2\,2\,3]$. A model of this order has $p = 120$ candidate terms.

To perform structure detection, estimates of the unknown system parameters and their statistics are needed. An estimate of unknown system parameters can be obtained using standard prediction error identification (PEI) techniques, such as extended least squares. Methods to obtain estimates of the parameter statistics for NARMAX models are discussed in Sec. IV.

III. Parameter Estimation

The structure detection procedure begins by computing an unbiased estimate of the unknown system parameters. Although NARMAX models provide a concise system representation, any noise on the output enters the model as product terms with the system input and output [17]. Consequently, most parameter estimation algorithms for linear systems cannot be applied directly because they assume that the noise terms in the model are independent [8,17].

Extended least squares (ELS) is one method, appropriate for NARMAX models, which easily enables unbiased estimates to be computed. ELS is a technique that addresses the bias problem by modeling the lagged errors to obtain unbiased parameter estimates. ELS for linear systems has been widely studied and is also referred to as Panuska's method, the extended matrix method, or approximate maximum likelihood [19–21].

In general, because the noise sequence is a realization of a stochastic process, it is not possible to solve for the noise source e, and it will not be equal to the prediction errors [17]. The prediction errors, $\hat{\boldsymbol{\epsilon}} \in \mathbb{R}^{N\times 1}$, are defined as

$$\hat{\boldsymbol{\epsilon}} = \mathbf{Z} - \hat{\mathbf{Z}} \quad (5)$$

where $\mathbf{Z} \in \mathbb{R}^{N\times 1}$ is the measured output and $\hat{\mathbf{Z}} = \Psi\hat{\boldsymbol{\theta}} \in \mathbb{R}^{N\times 1}$ is the predicted output. In ELS, the NARMAX formulation of Eq. (1) is redefined into a prediction error model by replacing e with $\hat{\epsilon}$, making it a deterministic least-squares problem.

The ELS formulation is defined as

$$\hat{\boldsymbol{\theta}} = (\Psi^T\Psi)^{-1}\Psi^T\mathbf{Z}, \quad \text{where } \Psi = [\Psi_{zu}\Psi_{zu\hat{\epsilon}}\Psi_{\hat{\epsilon}}] \quad (6)$$

$\hat{\boldsymbol{\theta}} \in \mathbb{R}^{p\times 1}$ is an ELS estimate of the system parameters, $\Psi \in \mathbb{R}^{N\times p}$ is a partitioned regressor matrix where Ψ_{zu} is a function of z and u only, $\Psi_{zu\hat{\epsilon}}$ represents all the cross products involving $\hat{\epsilon}$, and $\Psi_{\hat{\epsilon}}$ is a polynomial function of the prediction errors only [17].

Often, ELS is considered a pseudolinear approach to a parameter estimation [18,19,21]. Strictly speaking, the introduction of prediction errors into the model formulation no longer makes the model linear in the parameters because the prediction errors depend on the model output which is a function of all model parameters. The ELS technique solves a nonlinear optimization problem by ignoring the nonlinear character of the model and employing a least-squares approach. Essentially, ELS uses an approximate gradient of the model output with respect to the model parameters as a regression vector.

The prediction error method (PEM) is another approach to parameter estimation for nonlinear systems. PEM implements the true gradient to solve the nonlinear optimization problem. ELS is an approximation of PEM. In this paper, we chose to implement ELS over PEM because it does not require the computation of the true gradient. Computing the true gradient may be difficult in the general case where the objective is to learn about the true form of the underlying system.

Once an estimate of the system parameters is computed, an estimate of their statistics is needed to determine structure.

IV. Structure Detection

In system identification it is necessary to form estimates of the unknown parameters governing a random process, using a finite set of sample values. These can be computed using the ELS estimator. Parameter statistics are also needed to make a probability statement with respect to the unknown true parameter values. One such probability statement is to assign two limits to a parameter and assert that, with some specified probability, the true value of the parameter will be situated between those limits, which constitute the confidence interval.

Structure detection is concerned with how to best make a probability statement of the parameter estimates while maintaining an efficient (parsimonious) system description and yet complex enough to predict the system output. Many methods for structure detection have been proposed over the years. In this section, we discuss techniques appropriate for NARMAX modeling which are 1) easy to implement and 2) have previously shown promising results for polynomial NARMAX models. For a survey of the structure detection literature the reader is referred to [22].

A. *t* test

The t test in combination with regression analysis is sometimes referred to as a form of hypothesis testing by computing the differences between means [23]. In regression, the significance of each parameter estimate is checked using a statistical measure. If the model that was postulated is more general than needed, tests of the hypothesis are necessary to give a minimal model description.

Suppose the following model was fit:

$$E(\mathbf{Z}) = \hat{\theta}_1 + \hat{\theta}_2\psi_2 + \hat{\theta}_3\psi_3 + \cdots + \hat{\theta}_p\psi_p \tag{7}$$

The $\hat{\boldsymbol{\theta}}$s are tested against the null hypothesis, H_0, that $\hat{\theta}_i = 0$, $i = 1, 2, \ldots, p$. This allows the experimenter to assess which parameters are significant and which are not, and consequently which ones to retain.

Often in engineering applications, it is assumed that the errors are Gaussian independent, identically distributed (iid) variables. This assumption implies that $\mathbf{Z}$ will be Gaussian iid with mean $\Psi\boldsymbol{\theta}_0$ and variance $\sigma^2\mathbf{I}$,

$$\mathbf{Z} \in \mathcal{N}(\boldsymbol{\theta}_0, \sigma^2\mathbf{I}) \tag{8}$$

where $\mathcal{N}(\cdot)$ denotes the Gaussian (normal) distribution, $\boldsymbol{\theta}_0$ the true unknown parameter vector, σ^2 the variance, and $\mathbf{I}$ is an identity matrix of appropriate dimension [8]. The estimate $\hat{\boldsymbol{\theta}}$ is also Gaussian iid because it is a linear combination of $\mathbf{Z}$,

$$\hat{\boldsymbol{\theta}} \in \mathcal{N}(\boldsymbol{\theta}_0, \mathbf{P}) \tag{9}$$

where $\mathbf{P} = \sigma^2(\Psi^T\Psi)^{-1}$. Although the matrix $(\Psi^T\Psi)^{-1}$ is known to the user, σ^2 is typically not known, and must be estimated as

$$\hat{\sigma}^2 = \frac{1}{N-p}(\mathbf{Z} - \Psi\hat{\boldsymbol{\theta}})^T(\mathbf{Z} - \Psi\hat{\boldsymbol{\theta}}) \in \chi^2(N-p) \tag{10}$$

where $\chi^2(N-p)$ denotes the chi-squared distribution with $N-p$ degrees of freedom, and thus $\hat{\mathbf{P}} = \hat{\sigma}^2(\Psi^T\Psi)^{-1}$.

These estimates are easily calculated as a byproduct to the regression procedure and lend themselves to forming a confidence interval of the parameters via the student's t distribution, defined as the ratio of a normal random variable divided by the square root of a chi-squared random variable

$$t = \frac{\mathcal{N}\left(\hat{\boldsymbol{\theta}}_i, \hat{\mathbf{P}}\right)}{\sqrt{\hat{P}_{ii}}} \tag{11}$$

where $\hat{P}_{ii}$ denotes the ith diagonal element of $\hat{\mathbf{P}}$.

Specifically, the confidence interval for an estimate, $\hat{\theta}_i$, is

$$\hat{\theta}_i \pm t(\gamma/2, N-p)\hat{P}_{ii} \tag{12}$$

where t is the tabulated t ratio at the $\gamma/2$ level of significance ($0 \le \gamma \le 1$) with $N-p$ degrees of freedom. Therefore, the user is able to assess with $(1-\gamma)\%$ confidence that the parameter lies within this range. If the interval includes zero, it indicates that $\hat{\theta}_i$ is not significantly different from zero at the γ level and can be removed from the model.

This procedure assumes that an accurate estimate of parameter variances, that is, residuals, is available [6]. Although this assumption is violated for overparameterized models, structure detection of moderately overparameterized polynomial NARMAX models has shown good results [24].

B. Stepwise Regression

The stepwise regression algorithm is a widely used tool for computing model structure [25]. Stepwise regression relies on the incremental change in the residual sums of squares (RSS) resulting from adding or removing a parameter. Two Fisher–Snedecor distribution levels (F levels), F_{out} and F_{in}, are formed to determine whether a parameter should be removed from the model (F_{out}) or included in the model (F_{in}) [6,25–27]. These F levels are based on an F distribution with $N-p$ degrees of freedom for a predetermined γth level of significance. The statistics F_{in} and F_{out} are estimated from the residual sums of squares for a model with p parameters as

$$F_{\text{in}} = \frac{\text{RSS}_p - \text{RSS}_{p+1}}{\text{RSS}_{p+1}/(N-p-1)} \quad \text{and} \quad F_{\text{out}} = \frac{\text{RSS}_{p-1} - \text{RSS}_p}{\text{RSS}_p/(N-p)} \tag{13}$$

For good model parameterizations, F_{out} must not be greater than F_{in} [25–28].

This stepwise regression procedure can be summarized as follows [28].

1) Enter into the model any parameter(s) that are to be "forced" in.

2) Find the parameter from those not in the model but, available for inclusion, with the largest F_{in} value. If it is at least as great as a prespecified value of F_{in}, then add the parameter to the model. Stop if no parameter can be added.

3) Find the parameter among those in the model, other than those forced in, that has the smallest F_{out} value. If it is less than a prespecified value of F_{out}, then remove the parameter from the model. Repeat this step until no further parameter can be removed. Go to step 2.

It is well known that this method is sensitive to the order in which the regressors are introduced [26,29–31]; however, previous results for structure computation of polynomial NARMAX models have shown good results for simple models [24].

C. Bootstrap

Recently, the bootstrap has been shown to be a useful tool for structure detection of nonlinear models [24]. The bootstrap is a numerical method for estimating parameter statistics which requires few assumptions [32]. The conditions needed to apply bootstrap to least-squares estimation are quite mild, namely, that the errors be independent, identically distributed, and have zero mean.

The bootstrap is a technique to randomly reassign observations which enables reestimates of parameters to be computed. This randomization and computation of parameters is done numerous times and treated as repeated experiments. In essence, the bootstrap simulates a Monte Carlo analysis. For structure computation, the bootstrap method is used to detect spurious parameters, those parameters whose estimated values cannot be distinguished from zero.

Application of ELS to measured data gives the predicted model response $\hat{\mathbf{Z}}$, prediction errors $\hat{\epsilon}$, and parameter estimate $\hat{\boldsymbol{\theta}}$. A bootstrap version of the residuals, $\hat{\epsilon}^* = [\hat{\epsilon}_1^*, \hat{\epsilon}_2^*, \ldots, \hat{\epsilon}_N^*]$, is formed by random resampling, with replacement, of the estimated residuals $\hat{\epsilon} = [\hat{\epsilon}_1, \hat{\epsilon}_2, \ldots, \hat{\epsilon}_N]$. This resampling is accomplished by randomly selecting from $\hat{\epsilon}$ with an equal probability associated with each of the N elements. As an example of the bootstrap resampling process, consider a residual sequence with $N = 4$ data points. A possible bootstrap version of these residuals might be $\hat{\epsilon}^* = [\hat{\epsilon}_3, \hat{\epsilon}_1, \hat{\epsilon}_3, \hat{\epsilon}_2]$. These resampled errors are added to the model response to generate a bootstrap replication of the original data,

$$\mathbf{Z}^* = \Psi\hat{\boldsymbol{\theta}} + \hat{\epsilon}^* \tag{14}$$

This bootstrap sample, $\mathbf{Z}^*$, enables a new parameter estimate, $\hat{\boldsymbol{\theta}}^*$, to be computed This procedure is repeated B times to provide a set of parameter estimates from the B bootstrap replications,

$$\hat{\Theta}^* = \left[\hat{\boldsymbol{\theta}}_1^*, \ldots, \hat{\boldsymbol{\theta}}_B^*\right] \tag{15}$$

Parameter statistics are then easily computed from $\hat{\Theta}^*$ by forming percentile intervals at a chosen γ level of significance [24].

V. Nonlinear Structural Stiffness Model of Aircraft Dynamics

The dynamic aeroelastic equations governing pitch plunge can be described as

$$\begin{bmatrix} m & mx_\alpha b \\ mx_\alpha b & I_\alpha \end{bmatrix}\begin{bmatrix} \ddot{h} \\ \ddot{\alpha} \end{bmatrix} + \begin{bmatrix} c_h & 0 \\ 0 & c_\alpha \end{bmatrix}\begin{bmatrix} \dot{h} \\ \dot{\alpha} \end{bmatrix} + \begin{bmatrix} k_h & 0 \\ 0 & k_\alpha \end{bmatrix}\begin{bmatrix} h \\ \alpha \end{bmatrix} = \begin{bmatrix} -L \\ M \end{bmatrix} \tag{16}$$

where h denotes plunge motion, α pitch angle, x_α nondimensional distance between elastic axis and center of mass, m wing mass, I_α mass moment of inertia of the wing about the elastic axis, b semichord of the wing, $\{c_h, c_\alpha\}$ plunge and pitch structural damping coefficients, $\{k_h, k_\alpha\}$ plunge and pitch structural spring constants, and L, M aerodynamic lift and moment.

Typically, quasisteady aerodynamic forces and moments are assumed which can be modeled as

$$\begin{aligned} L &= \rho U^2 b c_{l_\alpha}\left[\alpha + \frac{\dot{h}}{U} + \left(\frac{1}{2} - a\right) b\frac{\dot{\alpha}}{U}\right] + \rho U^2 b c_{l_\beta}\beta \\ M &= \rho U^2 b^2 c_{m_\alpha}\left[\alpha + \frac{\dot{h}}{U} + \left(\frac{1}{2} - a\right) b\frac{\dot{\alpha}}{U}\right] + \rho U^2 b^2 c_{m_\beta}\beta \end{aligned} \tag{17}$$

where ρ denotes density of air, U free-stream velocity, c_{m_α}, c_{l_α} moment and lift coefficients per angle of attack, c_{m_β}, c_{l_β} moment and lift coefficient per control surface deflection, and a nondimensional distance from midchord to elastic axis. Combining Eqs. (16) and (17) gives the equations of motion as

$$\begin{aligned} &\begin{bmatrix} m & mx_\alpha b \\ mx_\alpha b & I_\alpha \end{bmatrix}\begin{bmatrix} \ddot{h} \\ \ddot{\alpha} \end{bmatrix} \\ &+ \begin{bmatrix} c_h + \rho U b c_{l_\alpha} & \rho U b^2 c_{l_\alpha}\left(\frac{1}{2} - a\right) \\ \rho U b^2 c_{m_\alpha} & c_\alpha - \rho U b^3 c_{m_\alpha}\left(\frac{1}{2} - a\right) \end{bmatrix}\begin{bmatrix} \dot{h} \\ \dot{\alpha} \end{bmatrix} \\ &+ \begin{bmatrix} k_h & \rho U^2 b c_{l_\alpha} \\ 0 & -\rho U^2 b^2 c_{m_\alpha} + k_\alpha \end{bmatrix}\begin{bmatrix} h \\ \alpha \end{bmatrix} = \begin{bmatrix} -\rho b c_{l_\beta} \\ \rho b^2 c_{m_\beta} \end{bmatrix} U^2\beta \end{aligned} \tag{18}$$

This model can be easily transformed to continuous-time state-space form to simulate a system response [33]. To transform these equations to state-space form, define the following:

$$\begin{aligned} \mathbf{M} &= \begin{bmatrix} m & mx_\alpha b \\ mx_\alpha b & I_\alpha \end{bmatrix} \\ \mathbf{C} &= \begin{bmatrix} c_h + \rho U b c_{l_\alpha} & \rho U b^2 c_{l_\alpha}\left(\frac{1}{2} - a\right) \\ \rho U b^2 c_{m_\alpha} & c_\alpha - \rho U b^3 c_{m_\alpha}\left(\frac{1}{2} - a\right) \end{bmatrix} \\ \mathbf{K} &= \begin{bmatrix} k_h & \rho U^2 b c_{l_\alpha} \\ 0 & -\rho U^2 b^2 c_{m_\alpha} + k_\alpha \end{bmatrix}, \qquad \mathbf{F} = \begin{bmatrix} -U^2\rho b c_{l_\beta} \\ U^2\rho b^2 c_{m_\beta} \end{bmatrix} \\ \mathbf{x} &= \begin{bmatrix} h \\ \alpha \end{bmatrix}, \qquad \mathbf{u} = \beta \end{aligned} \tag{19}$$

Substituting the definitions in Eq. (19) into Eq. (18) and combining terms gives a state-space formulation as

$$\begin{bmatrix} \dot{\mathbf{x}} \\ \ddot{\mathbf{x}} \end{bmatrix} = \begin{bmatrix} \mathbf{0} & \mathbf{I} \\ -\mathbf{M}^{-1}\mathbf{K} & -\mathbf{M}^{-1}\mathbf{C} \end{bmatrix}\begin{bmatrix} \mathbf{x} \\ \dot{\mathbf{x}} \end{bmatrix} + \begin{bmatrix} \mathbf{0} \\ -\mathbf{M}^{-1}\mathbf{F} \end{bmatrix}\mathbf{u} \tag{20}$$

This system representation provides both pitch and plunge accelerations. However, to save computational time, in the remainder of this paper we only consider plunge accelerations. Given a persistently exciting input, the results for the pitch component will be similar. In the subsequent development, we denote plunge acceleration ($\ddot{h}$) as z to conform to the notation used in Eqs. (1–14).

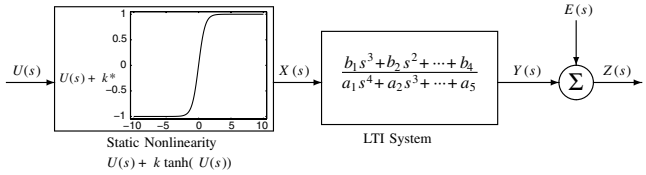

Fig. 1 Hammerstein model structure.

It has been observed that aeroelastic structures present a well-defined low frequency elastic mode composition [34,35]. Therefore, the linear modal components of this case example are represented using a fourth-order linear time-invariant (LTI) system [36].

Typically, an assumption is made that a structural nonlinearity exists in an aeroelastic system that affects not only flutter speed, but also the characteristics of the motion [37,38]. An example of an aeroelastic nonlinearity is a preloaded spring tab system. It has been proposed that this type of nonlinearity be modeled as a saturator [38]. In this paper, we chose to model this type of nonlinearity as a hyperbolic tangent, tanh(·), because a wing section response typically saturates smoothly.

Consider the model class given in Fig. 1. This blocked structured N-L model (static nonlinearity followed by a causal, linear, time-invariant, dynamic system) is commonly known as a Hammerstein model. Baldelli et al. [39] suggest that block oriented model structures, for example, Hammerstein models, are capable of representing the nonlinear behavior of most aeroelastic systems [40]. For this reason, the simulated aeroelastic example presented in this paper is a Hammerstein model, a static map represented by a hyperbolic tangent followed by a fourth-order LTI system.

A. Continuous to Discrete-Domain Approximations

A system's response is sampled via an analog to discrete converter [8]. As a result, many system representations are given in discrete time for identification and digital control synthesis.

Several methods exist for discretization of continuous-time infinite impulse response (IIR) systems. Most commonly used are Tustin's (also known as the bilinear transform), and zero-order hold (ZOH) methods; see, for example, [8,41,42]. Although both Tustin's and ZOH methods map the entire left-half s plane into the unit circle they do not offer the same model approximation. Tustin's method maps a proper continuous-time transfer function to a proper discrete-time transfer function but maps a strictly proper continuous-time transfer function also to a proper discrete-time transfer function. This often results in a large error in signal emulation due to loss of the inherent time delay (lagging effect). The ZOH explicitly accounts for the delay inherent in many continuous-time systems and provides for better signal emulation. Although Tustin's method can also provide good signal estimation for high sampling rates, it provides a model that is not intuitive. Models based on this approximation will include the current input as one of the model terms which may not be physically practical. For the aeroelastic system under investigation, the ZOH provides a system description that is both stable and intuitive. For these reasons ZOH is chosen to model the system dynamics.

B. Discrete-Time Representation of Nonlinear Structural Stiffness Model

The aeroelastic system in Fig. 1 is given in continuous time. In this section, we show how the model can be converted to discrete time and rewritten as a NARMAX model. To do so, we note that each block can be analyzed separately.

The first block representing the aeroelastic nonlinearity, as a hyperbolic tangent, is unchanged from continuous time to discrete time because it is a static map [8]. The second block characterizes the linear modal component of an aeroelastic system as a fourth-order LTI system and is converted to discrete time using the ZOH approximation [41]. In addition, we assumed the model is corrupted

by output additive (measurement) noise as

$$z(n) = y(n) + e(n) \tag{21}$$

where $z(n)$ is the noise corrupted output, $y(n)$ the unmeasured noise-free output, and $e(n)$ the measurement noise.

After collecting terms and combining, the overall nonlinear model was represented as a nonlinear difference equation with 16 terms as

$$\begin{aligned} z(n) &= \theta_1 z(n-1) + \theta_2 z(n-2) + \theta_3 z(n-3) + \theta_4 z(n-4) \\ &\quad + \theta_5 u(n-1) + \theta_6 u(n-2) + \theta_7 u(n-3) + \theta_8 u(n-4) \\ &\quad + \theta_9 \tanh[u(n-1)] + \theta_{10} \tanh[u(n-2)] + \theta_{11} \tanh[u(n-3)] \\ &\quad + \theta_{12} \tanh[u(n-4)] + \theta_{13} e(n-1) + \theta_{14} e(n-2) \\ &\quad + \theta_{15} e(n-3) + \theta_{16} e(n-4) + e(n) \end{aligned}$$

This is a NARMAX model because 1) it includes input–output terms that are combinations of linear and nonlinear terms and 2) it is linear in the parameters.

Structure detection can provide useful process insights that can be used in subsequent development or refinement of physical models. Therefore, in the sequel, we investigate 1) the performance of the algorithms outlined in Sec. IV on a simulated NARMAX model of aeroelastic structural stiffness and 2) applicability to experimental aircraft data.

VI. Simulation Protocol

The efficacy of the bootstrap, stepwise regression, and *t*-test structure detection algorithms was assessed using Monte Carlo simulations of a continuous-time model representing aeroelastic structural stiffness dynamics. The inputs were uniformly distributed, white, zero mean, random sequences with variances of 8 rad^2. One hundred Monte Carlo simulations were generated in which each input–output realization was unique and had a unique Gaussian white, zero mean, noise sequence added to the output. The output additive noise amplitude was increased in increments of 5 dB, from 20 to 5 dB signal-to-noise ratio (SNR). For identification, the data length was $N_e = [10,000\ 80,000]$ points and increased in increments of 10,000. For the bootstrap method, an initial estimate of the system parameters was computed and $B = 100$ bootstrap replications were generated to assess the distribution of each parameter. The number $B = 100$ was used because we have previously shown it is computationally inefficient to select large B, $B \gtrapprox 100$ [24,43]. For all three techniques, each parameter was tested for significance at the 95% confidence level and a backward elimination approach was implemented to reduce the fully parameterized model [23,24]. Specifically, using backward elimination, parameters of an overparameterizsed model were estimated and their significance tested to determine if they could be distinguished from zero. If the structure detection method indicated that the parameter(s) cannot be distinguished from zero, it/they were removed from the model. Next, the reduced model parameters and residuals were updated and tested again until convergence.

The model posed for structure computation was an additive nonlinear model of the form

$$z(n) = \sum_{v=1}^{q} \theta_v \psi(n) + \sum_{w=1}^{r} \theta_w f[\psi(n)] + e(n); \qquad q + r = p \tag{22}$$

The regressors posed for this identification problem were of the form given in Eq. (1), up to lag order 4, and the nonlinear mapping $f(\cdot)$ was chosen to be a hyperbolic tangent function [tanh(·)]; O= [4 4 4 tanh]. As previously stated, a tanh was selected as a basis because a wing section response is limited due to structural stiffness and appears to saturate smoothly. This gave a full model description with 27 candidate terms.

For each input–output realization, the structure detection result was classified into one of three categories:

Table 1 Continuous-time (CT) system coefficients

CT coefficient	Value
U	18.0 m/s
a	−0.600 m
b	0.135 m
I_α	0.065 m^2 Kg
k_h	2844 N/m
k_α	2.82 Nm/rad
x_a	0.247 m
c_h	27.4 Kg/s
c_α	0.180 m^2 Kg/s
ρ	1.23 kg/m^3
c_{l_α}	3.28
c_{l_β}	3.36
c_{m_α}	−0.628
c_{m_β}	−0.635
k	2

1) exact model: a model which contains only true system terms,

2) overmodeled: a model with all its true system terms plus spurious parameters, and

3) undermodeled: a model without all its true system terms. An undermodeled system may contain spurious terms as well.

The continuous-time values used in this study correspond to those found in experiments. The continuous-time parameters used in this study are shown in Table 1. Figure 2 presents a 50 s slice of a typical input–output data set used for this study. The left panel shows a uniform white input used as control surface deflection and the right panel shows the "measured" plunge acceleration response (5 dB SNR) superimposed on top of the noise-free plunge acceleration. Notice the input flap deflection (Fig. 2 left panel) is large (5 rads or ∼286 deg), and would not be possible for a real actuator. For this simulated example, an input of this amplitude was selected to provide good coverage for the tanh nonlinearity and to avoid rescaling. With experimental data a scaled nonlinearity is more appropriate to better conform to the data (see Sec. VII).

A. Simulation Results

Figure 3 shows the results of this study. The figures show the percent rate at which each structure detection algorithm selected the exact model, overmodeled and undermodeled for increasing data length and increasing SNR (decreasing noise amplitude).

The bootstrap technique had an approximately 0% rate of exact modeling for low SNR and small data length (5 dB SNR and $N_e = 10,000$–$20,000$), where undermodeling dominated with a rate of 100%. However, the rate of exact modeling increased linearly from 6 to 95% for $N_e = 10,000$–$80,000$ and 10–20 dB SNR. The rate of overmodeling was 0% for $N_e = 10,000$–$20,000$ at 5 dB SNR. For higher SNR (10–20 dB) and $N_e = 20,000$–$80,000$ the overmodeling rate decreased linearly from 42 to 5%. Although undermodeling dominated for low SNR and short data length, it decreased linearly from 48 to 0% for $N_e = 20,000$–$80,000$ and 10–20 dB SNR.

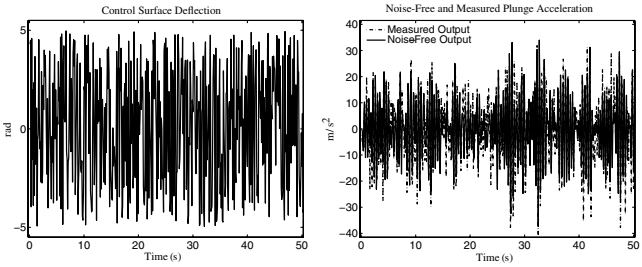

Fig. 2 Fifty second slice of a typical input–output data set used for structure computation. Left panel: Control surface deflection. Right panel: Measured (5 dB SNR) plunge acceleration output superimposed on top of noise-free plunge acceleration output.

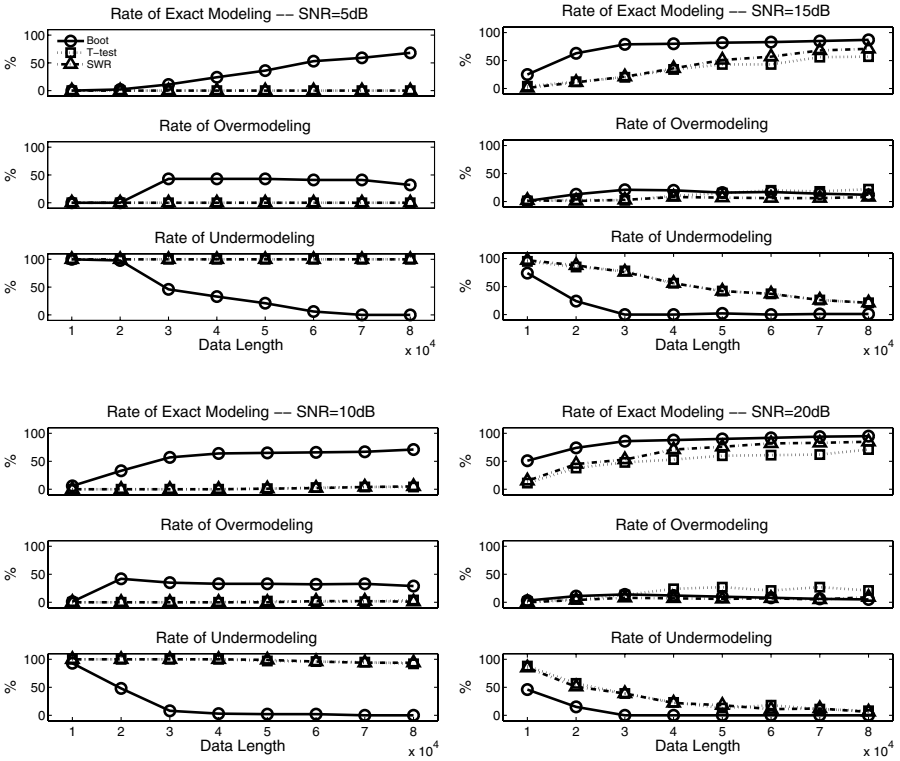

Fig. 3 Exact, over-, and undermodeling rate for a Hammerstein model describing aeroelastic dynamics: top panels: rate of exact modeling, center panels: rate of overmodeling, and bottom panel: rate of undermodeling. Ordinate: Percent selection. Abscissa: Data length.

For the stepwise regression method undermodeling dominated the structure computation effort for all data lengths for 5–10 dB SNR, with a rate of 100%. However, for high SNR levels, 15–20 dB, and $N_e = 10,000$–$80,000$ the undermodeling rate decreased from 97 to 6%. The rate of overmodeling was low for all SNRs and data lengths, ranging from a minimum of 0% to a maximum of 9%. The rate of selecting the exact model was constant at ∼0% for all data lengths and 5–10 dB SNR but increased from 1 to 85% for high SNR, 15–20 dB, and $N_e = 10,000$–$80,000$.

For the *t*-test approach undermodeling also dominated the structure computation effort with a rate of 100% for all data lengths at 5–10 dB SNR. For higher SNR levels (15–20 dB) and all data lengths, the undermodeling rate decreased linearly from 95 to 8%. The rate of overmodeling was ∼0% for all data lengths and 5–10 dB SNR. For higher SNRs of 15–20 dB, the rate of overmodeling remained approximately constant for all data lengths with a rate of ∼20%. The rate of selecting the exact model was constant at ∼0% for all data lengths and 5–10 dB SNR but increased from 4 to 70% for all data lengths and high SNR, 15–20 dB.

For this overparameterized model describing aeroelastic dynamics the bootstrap method clearly outperformed the *t* test and stepwise regression. As a result, in the subsequent section we implemented only the bootstrap structure detection method for the analysis of flight-test data.

VII. Structure Detection of Experimental AAW Data

Lastly, the applicability of using structure detection via a bootstrap approach for black-box modeling was assessed on experimental flight-test data from the F/A-18 AAW project at NASA Dryden Flight Research Center. The data analyzed for this study used collective aileron command input and structural accelerometer response output.

A. Procedures

Flight data were gathered during subsonic flutter clearance of the AAW. At each flight condition, the aircraft was subjected to multisine inputs corresponding to collective and differential aileron, collective and differential outboard leading edge flap, rudder, and collective stabilator excitations in the range of 3–35 Hz for 26 s. This paper considers accelerometer data measured during the collective aileron sweeps at Mach 0.85 at 4572 m (15,000 ft). The input collective aileron command was the exact signal sent by the onboard computer. The output was taken as the response of an accelerometer mounted near the left wing, outerfold aft. Data were sampled at 400 Hz. For analysis, the recorded flight-test data were decimated by a factor of 2, resulting in a final sampling rate of 200 Hz.

The system was identified applying the bootstrap approach, as outlined in Sec. VI except here scaled hyperbolic tangent functions were used because the input amplitude is less than ±1 (see Fig. 4). The scale factors used for the input, output, and error signals were in the range of $\nu = [0.1\ 1.0]$ and increased in increments of 0.1. A scaled hyperbolic tangent is denoted as $\tanh[\cdot, \nu]$. Models with every possible combination of scale factors were considered (i.e., structure computation was performed on 1000 models). The model which yielded the highest cross-validation percent fit was deemed the

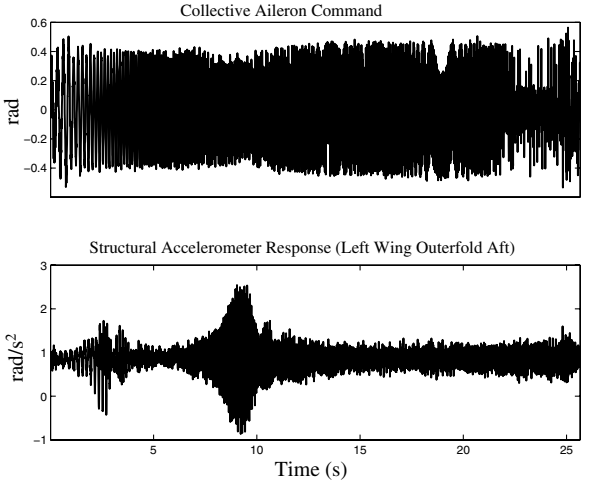

Fig. 4 Experimental F/A-18 AAW data. Upper panel: Recorded collective aileron position. Lower panel: Recorded structural accelerometer response (left wing outerfold aft).

best-fit model. For computation of a model structure, $N_e = 5200$ points were used from accelerometer response measurements on the left wing. To validate the computed model structure a cross-validation data set containing $N_v = 5200$ points was used from data collected at a similar location on the right wing.

B. Results

The results of identifying the AAW data are presented. Figure 4 shows the input–output trial used for this analysis. The data represent the collective aileron command sequence and structural accelerometer response (left wing, outerfold aft) used to compute the system structure.

Equation (23) depicts the model structure computed by the bootstrap method.

$$\begin{aligned} z(n) = {} & \hat{\theta}_0 + \theta_1 z(n-1) + \hat{\theta}_2 z(n-3) + \hat{\theta}_3 z(n-4) + \hat{\theta}_4 u(n) \\ & + \hat{\theta}_5 u(n-2) + \hat{\theta}_6 u(n-4) + \hat{\theta}_7 \tanh[u(n), 0.3] \\ & + \hat{\theta}_8 \tanh[u(n-1), 0.3] + \hat{\theta}_9 \tanh[u(n-3), 0.3] \\ & + \hat{\theta}_{10} \tanh[u(n-4), 0.3] + \hat{\theta}_{11} e(n-1) + \hat{\theta}_{12} e(n-3) \\ & + \hat{\theta}_{13} e(n-4) + e(n) \end{aligned} \tag{23}$$

The computed model structure is represented as a Hammerstein model with direct feedthrough terms and contains a total of 14 terms.

Figure 5 shows the predicted output for a cross-validation data set for the identified structure [Eq. (23)]. The upper panel displays the full 26 s time history of the accelerometer response recorded on the right wing outerfold aft. The lower panel displays a 10 s slice of the predicted output superimposed on top of the measured output which accounts for over 94% of the measured outputs variance. The result demonstrates that the computed model structure is capable of reproducing the measured output with high accuracy.

VIII. Discussion

A. Simulations

For the simulated model of aeroelastic structural stiffness dynamics, results demonstrated that for all SNR levels and sufficient data length ($N_e = 60,000$–$80,000$), the bootstrap method had a low rate of selecting an undermodeled model (2–0%) and a high rate of selecting the exact model (60–95%). However, the t test and stepwise regression both had difficulty computing the correct structure in this case study with a selection range of 3–70% and 2–85%, respectively, for equivalent data lengths and SNR levels. Moreover, both had a significantly higher rate of undermodeling, 100–6% and 100–8%, respectively.

Both the t test and stepwise regression had difficulty, but for different reasons. For the t test, extraneous parameters model the noise. This results in a biased estimate of the variance which may give models with incorrect structure. Stepwise regression also fails because it uses a F-ratio test to determine significance; this is sensitive to the order in which the terms are entered into the model and how much each term contributes to the output [24].

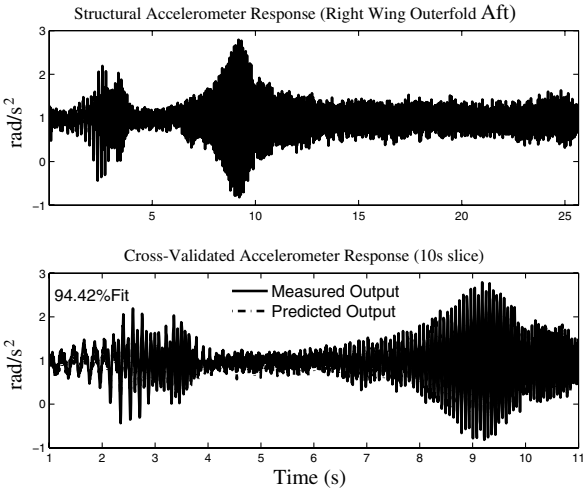

Fig. 5 Upper panel: Full time history of recorded structural accelerometer response (right wing, outerfold aft). Lower panel: Predicted accelerometer response of right wing outerfold aft superimposed on top of measured velocity output for the identified NARMAX AAW model from flight-test data $N_v = 5200$.

B. Experimental Aircraft Data

Experimental results demonstrate that structure computation as a tool for black-box modeling may be a useful tool for the analysis of dynamic aircraft data. The bootstrap successfully reduced the number of regressors posed to aircraft aeroelastic data yielding a parsimonious model structure. Additionally, this parsimonious structure was capable of predicting a large portion of the cross-validation data, collected on the adjacent wing and with a different sensor. This suggests that the identified structure and parameters explain the data well. Using percent fit alone as an indicator of model goodness could lead to incorrect interpretations of model validity. However, in many cases, for nonlinear models this may be the only indicator that is readily available.

For this study, only a hyperbolic tangent with fourth-order input, output, and error lag was used as a basis function to explain the nonlinear behavior of the F/A-18 AAW data. Clearly, different basis functions and a higher dynamic order (lag order) should be investigated to determine if another basis can produce accurate model predictions with reduced complexity. Moreover, further studies are necessary to evaluate whether the model structure is invariant under different operating conditions, such as Mach number and altitude, and model parameterizations.

C. Significance

This study illustrates the usefulness of structure detection as an approach to compute a parsimonious model of a highly complex nonlinear process, as demonstrated with experimental data of aircraft aeroelastic dynamics. Moreover, analysis of input–output data can provide useful process insights that can be used in subsequent development or refinement of physical models. In particular, morphological models are based on assumptions (e.g., these effects are important and those are negligible) which may be incorrect [44,45]. A structure computation approach to model identification may help uncover such surprises.

IX. Conclusions

Simulation results demonstrate that a bootstrap approach for structure computation of aircraft structural stiffness provided a high rate of true model selection. Although the t test and stepwise regression methods had difficulty providing accurate results for the system studied, they have previously been shown to provide reasonable results for polynomial class models. Using bootstrap, it is possible to compute good estimates of parameter statistics resulting in accurate estimates of model structure.

Moreover, this paper contributes to the understanding of the use of structure detection for modeling and identification of aerospace systems. These results may have practical significance in the analysis of aircraft dynamics during envelope expansion and could lead to more efficient control strategies. In addition, this technique could allow greater insight into the functionality of various systems dynamics, by providing a quantitative model which is easily interpretable.

Acknowledgments

This work was supported by grants from the National Academy of Sciences and the National Aeronautics and Space Administration (NASA), Dryden Flight Research Center, Aerostructures Branch (Grant No. NASA-NASW-99027).

References

[1] Leontaritis, I. J., and Billings, S. A., "Input-Output Parametric Models for Non-Linear Systems Part 1: Deterministic Non-Linear Systems," *International Journal of Control*, Vol. 41, No. 2, 1985, pp. 303–328.

[2] Leontaritis, I. J., and Billings, S. A., "Input-Output Parametric Models For Non-Linear Systems Part 2: Stochastic Non-Linear Systems," *International Journal of Control*, Vol. 41, No. 2, 1985, pp. 329–344.

[3] Unbehauen, H., "Some New Trends in Identification and Modeling of Nonlinear Dynamical Systems," *Applied Mathematics and Computation*, Vol. 78, No. 2, 1996, pp. 279–297.

[4] Billings, S. A., and Jones, G. N., "Orthogonal Least-Squares Parameter Estimation Algorithms for Non-Linear Stochastic Systems," *International Journal of Systems Science*, Vol. 23, No. 7, 1992, pp. 1019–1032.

[5] Freund, J. E., *Mathematical Statistics*, 1st ed., Prentice–Hall, Englewood Cliffs, NJ, 1962.

[6] Seber, G. A. F., *Linear Regression Analysis*, 1st ed., Wiley, New York, 1977.

[7] Ostrom, C. W., *Time Series Analysis: Regression Techniques*, 2nd ed., Sage Publications, Newberry Park, CA, 1990.

[8] Ljung, L., *System Identification: Theory for the User*, 2nd ed., Prentice–Hall, Englewood Cliffs, NJ, 1999.

[9] Kukreja, S. L., and Brenner, M. J., "Nonlinear Aeroelastic System Identification with Application to Experimental Data," *Journal of Guidance, Control, and Dynamics*, Vol. 29, No. 2, 2006, pp. 374–381.

[10] O'Neil, T., Gilliatt, H. C., and Strganac, T. W., "Investigations of Aeroelastic Response for a System with Continuous Structural Nonlinearities," AIAA Paper 96-1390, April 1996, p. 1390.

[11] O'Neil, T., and Strganac, T. W., "Nonlinear Aeroelastic Response—Analyses and Experiments," AIAA Paper 96-1390, April 1996, p. 0014.

[12] Harris, C. J., and Billings, S. A., *Self Tuning and Adaptive Control: Theory and Applications*, 2nd ed., Peter Peregrinus, London, 1985.

[13] Eykhoff, P., *System Identification*, 1st ed., Wiley, New York, 1974.

[14] Chen, S., and Billings, S. A., "Representations of Non-Linear Systems: The NARMAX Model," *International Journal of Control*, Vol. 49, No. 3, 1989, pp. 1013–1032.

[15] Billings, S. A., and Chen, S., "Extended Model Set, Global Data and Threshold Model Identification of Severely Non-Linear Systems," *International Journal of Control*, Vol. 50, No. 5, 1989, pp. 1897–1923.

[16] Beck, J. V., and Arnold, K. J., *Parameter Estimation in Engineering and Science*, Probability and Mathematical Statistics, Wiley, New York, 1977.

[17] Billings, S. A., and Voon, W. S. F., "Least Squares Parameter Estimation Algorithms for Non-Linear Systems," *International Journal of Systems Science*, Vol. 15, No. 6, 1984, pp. 601–615.

[18] Goodwin, G. C., and Payne, R. L., *Dynamic System Identification: Experiment Design and Data Analysis*, Vol. 136, Mathematics in Science and Engineering, Academic Press, New York, 1977.

[19] Panuska, V., "A Stochastic Approximation Method for Identification of Linear Systems Using Adaptive Filtering," *Proceedings of the 9th Joint Automatic Control Conference*, IEEE, Ann Arbor, MI, June 1968, pp. 1014–1021.

[20] Panuska, V., "An Adaptive Recursive Least Squares Identification Algorithm," *Proceedings of the 8th IEEE Symposium on Adaptive Processes*, IEEE, University Park, PA, Nov. 1969, page paper 6e.

[21] Young, P. C., "The Use of Linear Regression and Relaxed Procedures for the Identification of Dynamic Processes," *Proceedings of the 7th IEEE Symposium on Adaptive Processes*, IEEE, Los Angeles, CA, Dec. 1968, pp. 501–505.

[22] Haber, R., and Unbehauen, H., "Structure Identification of Nonlinear Dynamic Systems—A Survey on Input/Output Approaches," *Automatica*, Vol. 26, No. 4, 1990, pp. 651–677.

[23] Draper, N. R., and Smith, H., *Applied Regression Analysis*, 2nd ed., Wiley, New York, 1981.

[24] Kukreja, S. L., Galiana, H. L., and Kearney, R. E., "A Bootstrap Method for Structure Detection of NARMAX Models," *International Journal of Control*, Vol. 77, No. 2, 2004, pp. 132–143.

[25] Efroymson, M. A., *Multiple Regression and Correlation. in Mathematical Methods for Digital Computers*, 1st ed., Wiley, New York, 1960.

[26] Sjöberg, J., Zhang, Q., Ljung, L., Delyon, B., Benveniste, A., Glorennec, P. Y., Hjalmarsson, H., and Juditsky, A., Nonlinear Black-Box Modeling in System Identification: A Unified Overview, *Automatica*, Vol. 31, No. 12, 1995, pp. 1691–1724.

[27] Smillie, K. W., *An Introduction to Regression and Correlation*, 1st ed., Academic Press, London, 1966.

[28] Miller, A. J., "The Convergence of Efroymson's Stepwise Regression Algorithm," *The American Statistician*, Vol. 50, No. 2, 1996, pp. 180–181.

[29] Copas, J. B., "Regression, Prediction and Shrinkage," *Journal of the Royal Statistical Society B*, Vol. 45, No. 2, 1983, pp. 311–354.

[30] Hurvich, C. M., and Tsai, C. L., "The Impact of Model Selection on Inference in Linear Regression," *The American Statistician*, Vol. 44, No. 3, 1990, pp. 214–217.

[31] Mantel, M., "Why Stepdown Procedures in Variable Selection," *Technometrics*, Vol. 12, No. 3, 1970, pp. 621–625.

[32] Efron, B., "Computer and the Theory of Statistics: Thinking the Unthinkable," *SIAM Review*, Vol. 21, No. 4, 1979, pp. 460–480.

[33] Lind, R., and Brenner, M. J., *Robust Aeroservoelastic Stability Analysis: Flight Test Applications*, 1st ed., Springer–Verlag, New York, 1999.

[34] Gawronski, W., *Balanced Control of Flexible Structures*, 1st ed., Springer–Verlag, London, 1996.

[35] Smith, R., "Eigenvalue Perturbation Models for Robust Control," *IEEE Automatic Control*, Vol. 40, No. 6, 1995, pp. 10631–1066.

[36] Baldelli, D. H., Chen, P. C., Liu, D. D., Lind, R., and Brenner, M., "Nonlinear Aeroelastic Modeling by Block-Oriented Identification," AIAA Paper 2004-1938, 2004.

[37] Dowell, E. H., Edwards, J., and Strganac, T., "Nonlinear Aeroelasticity," *AIAA Journal of Aircraft*, Vol. 40, No. 1, 2003, pp. 857–874.

[38] Lee, B. H. K., Pricei, S. J., and Wong, Y. S., "Nonlinear Aeroelastic Analysis of Airfoils: Bifurcation and Chaos," *Progress in Aerospace Sciences*, Vol. 35, No. 3, 1999, pp. 205–334.

[39] Baldelli, D. H., Mazzaro, M. C., and Śanchez Peña, R. S., "Robust Identification of Lightly Damped Flexible Structures by Means of Orthonormal Bases," *IEEE Transactions on Control Systems Technology*, Vol. 9, No. 5, 2001, pp. 696–707.

[40] Palanthandalam-Madapusi, H. J., Hoagg, J. B., and Berstein, D. S., "Basis-Function Optimization for Subspace-Based Nonlinear Identification of Systems with Measured-Input Nonlinearities," *Proceedings of the IEEE American Control Conference*, Vol. 5, IEEE, Piscataway, NJ, July 2004, pp. 4788–4793.

[41] Åström, K. J., and Wittenmark, B., *Computer-Controlled Systems: Theory and Design*, 3rd ed., Prentice–Hall, Englewood Cliffs, NJ, 1996.

[42] Franklin, G. F., Powell, J. D., and Emami-Naeini, A., *Feedback Control of Dynamic Systems*, 4th ed., Addison Wesley, New York, 2002.

[43] Kukreja, S. L., "A Suboptimal Bootstrap Method for Structure Detection of Nonlinear Output-Error Models, *Proceedings of the 13th IFAC Symposium System Identification*, Vol. 13, IFAC, Laxenburg, Austria, Aug. 2003, pp. 1566–1571.

[44] Pearson, R. K., "Nonlinear Input/Output Modelling," *Journal of Process Control*, Vol. 5, No. 4, 1995, pp. 197–211.

[45] Pottmann, M., and Pearson, R. K., "Block-Oriented NARMAX Models with Output Multiplicities," *AIChE Journal*, Vol. 44, No. 1, 1998, pp. 131–140.